Available online at www.sciencedirect.com
SCIENCE DIRECT
Journal of Molecular Catalysis A: Chemical 254 (2006) 20–28
JOURNAL OF MOLECULAR CATALYSIS A: CHEMICAL
www.elsevier.com/locate/molcata

Generation of *trans*-spanning diphosphine ligands via alkene metathesis: Synthesis, structure, and dynamic behavior of a missing link in a series of square-planar platinum complexes

Natascha Lewanzik [a], Thomas Oeser [a], Janet Blümel [a,*], John A. Gladysz [b,*]

[a] *Department of Organic Chemistry, University of Heidelberg, Im Neuenheimer Feld 270, 69120 Heidelberg, Germany*
[b] *Institut für Organische Chemie, Friedrich-Alexander-Universität Erlangen-Nürnberg, Henkestraße 42, 91054 Erlangen, Germany*

Available online 8 May 2006

Abstract

Reaction of $KPPh_2$ and $Br(CH_2)_5CH{=}CH_2$ gives the phosphine $PPh_2(CH_2)_5CH{=}CH_2$ (89%), which is treated with the platinum tetrahydrothiophene complex $[Pt(\mu\text{-}Cl)(C_6F_5)(S(CH_2CH_2{-})_2)]_2$ to yield *trans*-$(Cl)(C_6F_5)Pt(PPh_2(CH_2)_5CH{=}CH_2)_2$ (**4b**, 80%). Ring-closing alkene metathesis (Grubbs' catalyst) gives *trans*-$(Cl)(C_6F_5)Pt(PPh_2(CH_2)_5CH{=}CH(CH_2)_5PPh_2)$ (**5b**, 84%), which features a *trans*-spanning diphosphine ligand. The *Z*/*E* C=C mixture is hydrogenated (1 atm, 10% Pd/C) to give *trans*-$(Cl)(C_6F_5)Pt(PPh_2(CH_2)_{12}PPh_2)$ (**6b**, 99%). The crystal structures of **4b** and (*Z*)-**5b** are determined. In the former, both $(CH_2)_5CH{=}CH_2$ moieties are directed on the same side of the platinum square plane. Low temperature ^{13}C NMR spectra of **6b** show two sets of signals for the diastereotopic P*Ph*$_2$ groups. These coalesce upon warming, which requires the passage of the chloride ligand through the macrocycle. Analysis by the complete bandwidth method gives $\Delta H^{\ddagger}$ and $\Delta S^{\ddagger}$ values of 6.0 ± 0.4 kcal mol^{-1} and -13.9 ± 2.6 eu. The ^{31}P, ^{13}C, and ^{2}H CP/MAS NMR spectra of polycrystalline **6b** and **6b**-d_2 are studied, and indicate appreciable conformational mobility of the methylene chain in the solid state.
© 2006 Elsevier B.V. All rights reserved.

Keywords: Alkene/olefin metathesis; Hydrogenation; Platinum; Macrocycle; Rotational barrier; Dynamic NMR; Solid-state NMR; Molecular rotor

1. Introduction

This paper is part of a collection of articles describing developments reported at the 16th International Symposium on Olefin Metathesis and Related Chemistry, which was held August 7–12 in Poznań, Poland. One prominent theme was the emergence of alkene metathesis, particularly with the Grubbs' catalyst family, for the synthesis of architecturally sophisticated organometallic compounds [1,2]. In this context, we have shown that a variety of complexes that contain *trans*-phosphine ligands with one or more substituents of the formula $(CH_2)_nCH{=}CH_2$ ($n \geq 4$) undergo efficient ring-closing metathesis [3–5]. The macrocyclic products feature *trans*-spanning diphosphine ligands [6]. In nearly all cases, the C=C linkages can be cleanly hydrogenated. Schemes 1 and 2 illustrate sequences leading to the triply bridged iron tricarbonyl complexes **2a**–**c** [5] and the singly bridged platinum complexes **6a**,**c**,**e**–**f** [3].

When the bridges connecting the phosphorus atoms are long enough, and the central L_nM fragments are small enough, such compounds can be viewed as molecular rotors [7]. The symmetries of the iron complexes **2** are too high for $Fe(CO)_3$ rotation to be probed by conventional solution NMR techniques. However, the corresponding $Fe(CO)_2(NO)^+$ complexes **3** [5] are ideal. The ^{13}C NMR spectrum of **3b**, which features 12 methylene groups in each bridge, showed two sets of methylene signals (2:1) at room temperature. These coalesced at elevated temperature. The ^{13}C NMR spectrum of **3c**, which features 14 methylene groups in each bridge, showed only one set of methylene signals at room temperature. This decoalesced to two sets at low temperature. Complete bandwidth analysis gave $\Delta H^{\ddagger}$ and $\Delta S^{\ddagger}$ values of 9.5 kcal mol^{-1} and -6.5 eu for $Fe(CO)_2(NO)^+$ rotation. Pathways involving ligand dissociation could be excluded.

Unfortunately, in the case of the singly bridged platinum complexes **6a**,**c**,**e**–**f**, no rotational barriers could be determined [3]. As illustrated in Scheme 3, the P*Ph*$_2$ groups and PC*H*$_2$ protons of **6** are diastereotopic. When the bridge is sufficiently long, the smaller chloride ligand can pass underneath, and the groups

* Corresponding authors.
E-mail addresses: gladysz@organik.uni-erlangen.de (J.A. Gladysz), j.bluemel@urz.uni-heidelberg.de (J. Blümel).

1381-1169/$ – see front matter © 2006 Elsevier B.V. All rights reserved.
doi:10.1016/j.molcata.2005.12.047

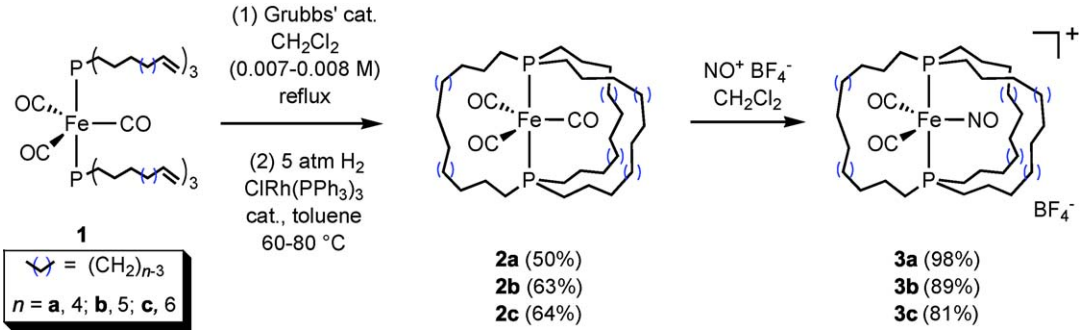

Scheme 1. Iron carbonyl complexes with *trans*-spanning diphosphine ligands.

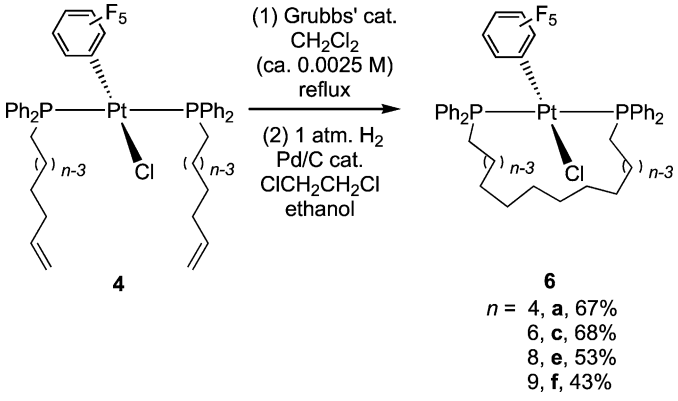

Scheme 2. Previously synthesized platinum complexes with *trans*-spanning diphosphine ligands.

are rendered equivalent [8]. When this process is rapid enough, the corresponding signals will coalesce. For **6a**, which features 10 methylene groups in the bridge, two sets of P*Ph*$_2$ ^{13}C NMR signals were observed at room temperature. These did not coalesce at 95 °C in toluene-d_8. Application of the coalescence formula allowed a lower limit of 17.4 kcal/mol ($\Delta G^{\ddagger}$, 95 °C) to be placed upon the barrier. With **6c**, which features 14 methylene groups in the bridge, only one set of signals was observed at room temperature. No decoalescence occurred at −90 °C in THF-d_8. From these data, an upper limit of 8.4 kcal/mol could be estimated for the barrier.

In order to better design related platinum-based molecular rotors, it was desirable to obtain an exact barrier for a member of this series of molecules. Hence, we set out to synthesize and study the variable temperature NMR spectra of the missing link **6b**, with 12 methylene groups in each bridge. In this paper, we report the successful realization of these objectives, as well as (a) crystal structures of two precursor complexes that exhibit several surprising features, and (b) multinuclear solid-state CP/MAS NMR data for polycrystalline **6b** and a dideutero derivative **6b**-d_2 that provide further information on dynamic properties.

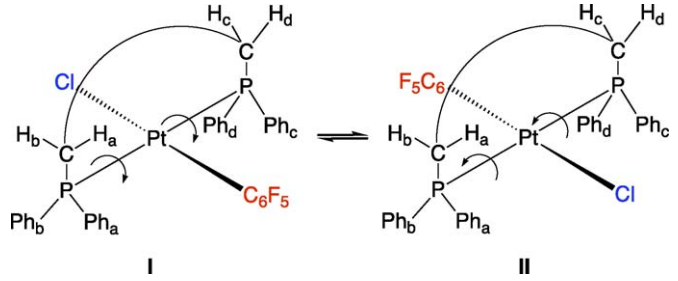

Scheme 3. Exchange of diastereotopic groups in platinum complexes **6**.

2. Results

2.1. Syntheses

As expected from similar procedures described earlier [3], reaction of $KPPh_2$ and the α,ω-bromoalkene $Br(CH_2)_5CH{=}CH_2$ gave $PPh_2(CH_2)_5CH{=}CH_2$ in 89% yield. As shown in Scheme 4, this phosphine was combined with the platinum tetrahydrothiophene complex $[Pt(\mu\text{-}Cl)(C_6F_5)(S(CH_2CH_2{-})_2)]_2$ [9] under

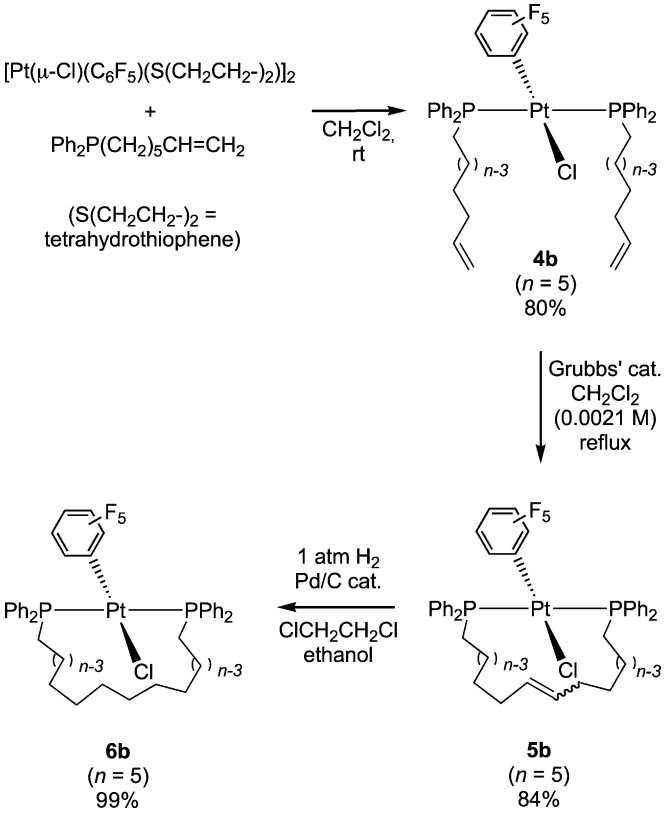

Scheme 4. Syntheses of new platinum complexes with *trans*-spanning diphosphine ligands.

conditions analogous to those previously used for the synthesis of **4a**,**c**,**e**–**f**. Workup gave the bis(phosphine) complex *trans*-(Cl)(C_6F_5)Pt($PPh_2(CH_2)_5CH{=}CH_2$)$_2$ (**4b**) as a white solid in 80% yield, which was characterized by NMR (^{1}H, ^{13}C, ^{31}P, ^{19}F) and IR spectroscopy and mass spectrometry as summarized in Section 4. All properties were similar to those of **4a**,**c**,**e**–**f**. As expected, the enantiotopic P*Ph*$_2$ groups gave a single set of ^{13}C NMR signals, most of which were triplets due to virtual coupling to both phosphorus nuclei [10]. The original NMR spectra for all new compounds in this paper have been depicted elsewhere [11].

Alkene metathesis was conducted under conditions analogous to those used in Scheme 2. As shown in Scheme 4, CH_2Cl_2 solutions of **4b** (ca. 0.0021 M) and Grubbs' catalyst (8 mol%, added in three portions) were refluxed for 5 h. Workup gave the crude macrocycle *trans*-(Cl)(C_6F_5)Pt($PPh_2(CH_2)_5CH{=}CH(CH_2)_5PPh_2$) (**5b**) in 84% yield. The ^{31}P NMR spectrum indicated a 74:26 mixture of C=C isomers. Based upon the calculated values of the chemical shifts of the =CH ^{1}H NMR signals, and the crystal structure below, the major isomer is tentatively proposed to be *Z* (*cis*). Subsequent hydrogenation (1 atm, 10% Pd/C catalyst) gave the title complex *trans*-(Cl)(C_6F_5)Pt($PPh_2(CH_2)_{12}PPh_2$) (**6b**) in 99% yield. This material was characterized analogously to **4b**. The diastereotopic *PPh*$_2$ groups gave a single set of ^{13}C NMR signals.

In order to prepare a substrate for a solid-state NMR experiment below, the preceding reaction was repeated with D_2. The ^{13}C{^{1}H, ^{31}P} NMR spectrum of the resulting **6b**-d_2 showed that deuterium had also been incorporated into what would correspond to the allylic position of **5b**. This suggested a competing C=C isomerization. Accordingly, an analogous reaction was conducted with Wilkinson's catalyst. The resulting **6b**-d_2 showed only a single ^{13}C NMR signal with a directly bound deuterium atom, and a single ^{2}H NMR signal.

2.2. Crystal structures

The crystal structures of **6a**,**c**,**e**–**f** have been reported previously. However, no data on the precursors **4a**,**c**–**e** or **5a**,**c**,**e**–**f** have heretofore been available. Interestingly, single crystals of **4b** could be obtained from CH_2Cl_2/ethanol. X-ray data were collected as summarized in Table 1 and Section 4. Refinement revealed considerable disorder, involving both $(CH_2)_4CH{=}CH_2$ moieties, one PPh_2 moiety, and certain C_6F_5 fluorine atoms. Nonetheless, the structure could be solved, and a representative conformation is depicted in Fig. 1. The other conformations were similar, and the structure is further analyzed below.

A crystal of **5b** was also obtained from CH_2Cl_2/ethanol. X-ray data were collected, and refinement gave the *cis* or *Z* structure shown in Fig. 2. However, NMR spectra showed the presence of both C=C isomers in the sample (74:26). Key metrical parameters for **4b** and (*Z*)-**5b** are summarized in Table 2. In each case, stacking interactions involving the pentafluorophenyl ligand and a phenyl group on each phosphorus are evident. The averages of the two centroid–centroid distances are 3.76 Å (**4b**) and 4.05 Å ((*Z*)-**5b**). In (*Z*)-**5b**, the distances from the platinum atom to the most remote carbon atoms of the macrocycle, C(54), C(55),

Table 1
Summary of crystallographic data

Compound	**4b**	(*Z*)-**5b**
Empirical formula	$C_{44}H_{46}ClF_5P_2Pt$	$C_{42}H_{42}ClF_5P_2Pt$
Formula weight	962.29	934.24
Temperature (K)	200(2)	200(2)
Wavelength (Å)	0.71073	0.71073
Crystal system	Monoclinic	Monoclinic
Space group	$P2_1/n$	$C2/c$
Unit cell dimensions		
a (Å)	11.033(2)	39.173(6)
b (Å)	14.841(2)	11.071(2)
c (Å)	25.864(4)	20.367(3)
β (°)	98.817(3)	117.454(4)
Volume (Å^3)	4185(1)	7838(2)
Z	4	8
ρ_{calc} (g/cm^3)	1.53	1.58
μ (mm^{-1})	3.54	3.78
Max. and min. transmission	0.68 and 0.50	0.86 and 0.64
Crystal size (mm^3)	0.23 × 0.20 × 0.12	0.13 × 0.09 × 0.04
θ limit (°)	2.4–24.7	2.4–22.0
Index ranges (h; k; l)	−12, 12; −17, 17; −30, 30	−41, 41; −11, 11; −21, 21
Reflections collected	32011	23153
Independent reflections	7053 [R(int) = 0.039]	4762 [R(int) = 0.073]
Observed reflections [$I > 2\sigma(I)$]	5592	4063
Data/restraints/parameters	7053/48/473	4762/0/480
Goodness-of-fit on F^2	1.04	1.10
Final R indices [$I > 2\sigma(I)$]	R_1 = 0.046, ωR_2 = 0.104	R_1 = 0.040, ωR_2 = 0.080
Largest diff. peak and hole (eÅ^{-3})	2.88 and −2.02	0.57 and −1.57

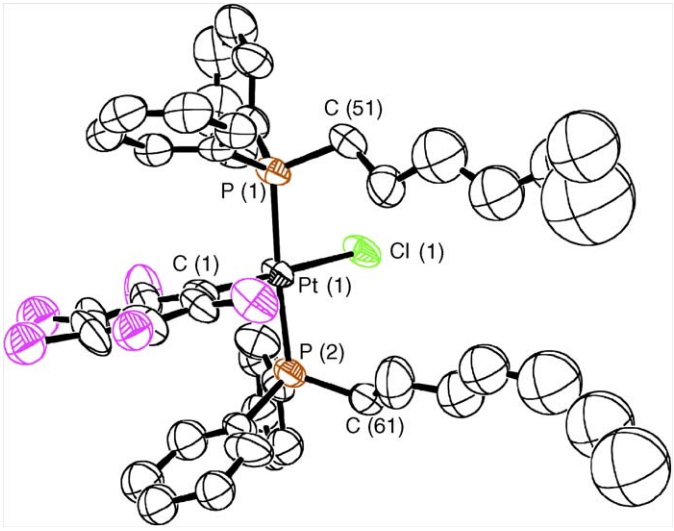

Fig. 1. Molecular structure of **4b** (one of several disordered conformations; see text).

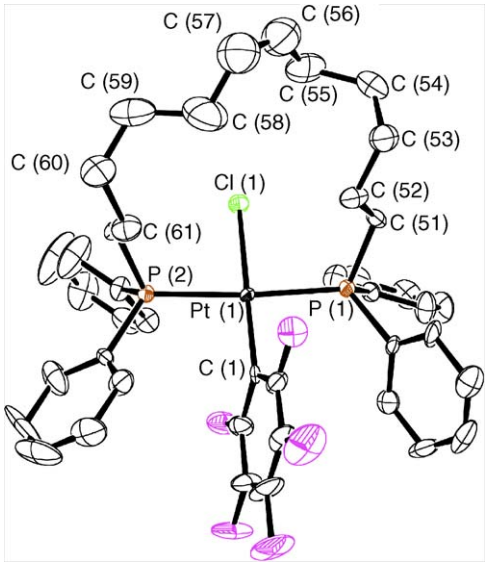

Fig. 2. Molecular structure of (*Z*)-**5b**.

C(56), C(57), C(58), and C(59), were 5.61, 5.38, 6.21, 6.17, 5.15, and 5.55 Å, respectively.

2.3. Solution NMR studies

As noted in the introduction, the ^{13}C NMR spectra of the 17–23-membered macrocycles **6c–e** (Scheme 2) gave only a single set of PPh_2 signals, whereas that of the 13-membered macrocycle **6a** gave two sets. This indicates that the chloride ligands rapidly pass underneath the methylene chains of the *trans*-spanning diphosphine ligands in **6c–e** on the NMR time scale (Scheme 3). Complex **6b** similarly gave a single set of ^{13}C NMR signals for the P*Ph*$_2$ groups at room temperature. At −95 °C in THF-d_8, the signals broadened, but did not decoalesce. No decoalescence phenomena were observed when ^{1}H NMR spectra were recorded at −95 °C.

^{13}C NMR spectra were therefore recorded in $CDFCl_2$ [12], which has a lower melting point than THF-d_8 (−135 °C versus −108 °C), between room temperature and −110 °C (163 K). Two limiting spectra are shown in Fig. 3. The signals for the *ortho*, *para*, and *meta* carbon atoms in the higher temperature spectrum (bottom; ca. 132.8, 130.4, and 128.1 ppm) decoalesced into two sets (top). This process is traced by the spectra in Fig. 4, which furthermore illustrate a moderate temperature dependence of the chemical shifts. The evolution of the weaker and more strongly coupled signal for the *ipso* carbon atoms is obscured by the noise and other signals. At the low temperature limit, the splittings of the *para* and *meta* signals (1.9 and 1.2 ppm or 191 and 121 Hz) are less than that of the *ortho* signals (4.3 ppm or 433 Hz).

The spectra in Fig. 4 (left) were simulated using the Complete Bandshape Simulation (CBS) routine of the program gNMR 4.1 (right) [13]. The simulation of the spectrum in Fig. 3 is shown elsewhere [11]. The overall agreement was reasonably satisfying, and rate constants could be calculated at each temperature. An Eyring plot gave $\Delta H^{\ddagger}$ and $\Delta S^{\ddagger}$ values of 6.0 ± 0.4 kcal mol^{-1} and -13.9 ± 2.6 eu for the process that renders the P*Ph*$_2$ groups equivalent. The virtual coupling of the *ipso*, *ortho*, and *meta* signals to both phosphorus nuclei at the high-temperature limit excludes mechanisms involving phosphine dissociation. The ^{31}P NMR signal also remains coupled to platinum at the high-temperature limit $^{1}J_{PPt}$ = 2683 Hz).

Table 2
Key bond lengths, bond angles, and torsion angles

Complex	**4b**[a]	(*Z*)-**5b**
Bond lengths (Å)		
Pt(1)—P(1)	2.302(2)	2.307(2)
Pt(1)—P(2)	2.300(2)	2.314(2)
Pt(1)—Cl(1)	2.365(2)	2.364(2)
Pt(1)—C(1)	2.014(7)	2.004(7)
P(1)—C(51)	1.818(7)	1.820(7)
P(2)—C(61)/C(62)	1.819(8)	1.812(7)
C(51)—C(52)	1.53(1)	1.53(1)
C(52)—C(53)	–	1.52(1)
C(53)—C(54)	–	1.52(1)
C(54)—C(55)	–	1.54(1)
C(55)—C(56)	–	1.50(1)
C(56)—C(57)	–	1.30(1)
C(57)—C(58)	–	1.47(2)
C(58)—C(59)	–	1.58(1)
C(59)—C(60)	–	1.49(1)
C(60)—C(61)	–	1.54(1)
C(61)—C(62)	1.50(1)	1.52(1)
Bond angles (°)		
C(1)—Pt(1)—P(1)	91.6(2)	90.6(2)
C(1)—Pt(1)—P(2)	90.2(2)	94.7(2)
P(1)—Pt(1)—P(2)	175.12(7)	174.69(7)
C(1)—Pt(1)—Cl(1)	177.7(2)	178.7(2)
P(1)—Pt(1)—Cl(1)	89.70(6)	89.19(7)
P(2)—Pt(1)—Cl(1)	88.57(6)	85.55(7)
C(55)—C(56)—C(57)	–	132(1)
C(56)—C(57)—C(58)	–	126(1)
Torsion angles (°)		
P(2)—Pt(1)—P(1)—C(51)	–	57.4(8)
Pt(1)—P(1)—C(51)—C(52)	–	46.3(6)
P(1)—C(51)—C(52)—C(53)	–	175.2(6)
C(51)—C(52)—C(53)—C(54)	–	61(1)
C(52)—C(53)—C(54)—C(55)	–	63(1)
C(53)—C(54)—C(55)—C(56)	–	70(1)
C(54)—C(55)—C(56)—C(57)	–	−114(1)
C(55)—C(56)—C(57)—C(58)	–	4(2)
C(56)—C(57)—C(58)—C(59)	–	−117(1)
C(57)—C(58)—C(59)—C(60)	–	−165(1)
C(58)—C(59)—C(60)—C(61)	–	−53(1)
C(59)—C(60)—C(61)—C(62)	–	−75(1)
C(60)—C(61)—C(62)—P(2)	–	−178.9(6)
C(61)—C(62)—P(2)—Pt(1)	–	66.7(6)
C(62)—P(2)—Pt(1)—P(1)	–	65.3(8)

[a] Several disordered conformations are present in the crystal; see text.

2.4. Solid-state NMR studies

The wideline ^{31}P CP NMR spectrum of **6b** was measured first (depicted elsewhere [11]). The chemical shift anisotropy (CSA) [14] was typical for polycrystalline metal complexes with two phosphine ligands. The span (δ_{11}–δ_{33}) of the signal amounted

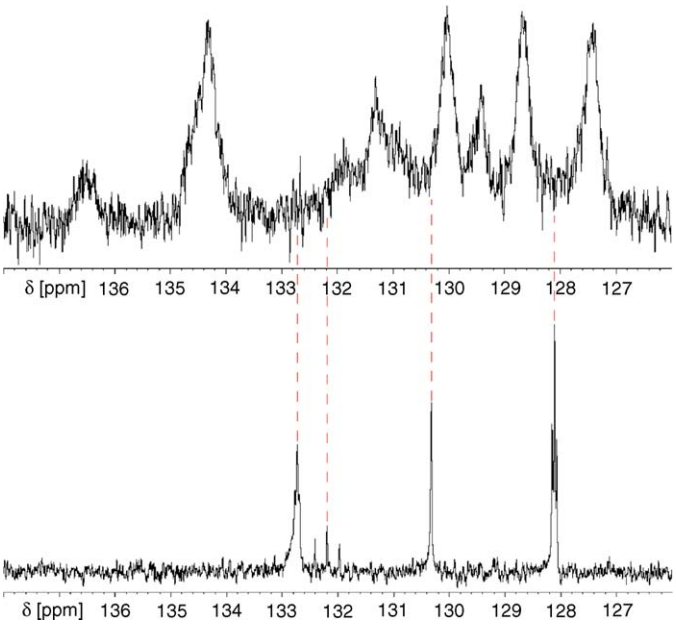

Fig. 3. ^{13}C NMR spectra of **6b** in $CDFCl_2$ (100.6 MHz, aromatic region only). Top, 163 K; bottom, 273 K.

to 125 ppm, with $\delta_{11} = 85.1$, $\delta_{22} = 13.2$, and $\delta_{33} = -31.0$ ppm. From these data, an isotropic chemical shift of 13.6 ppm could be calculated ($\delta_{iso} = 1/3(\delta_{11} + \delta_{22} + \delta_{33})$), which in turn allowed the asymmetry parameter η of 0.25 to be calculated ($\eta = (\delta_{22} - \delta_{33})/(\delta_{11} - \delta_{iso})$) [14]. Fig. 5 shows the ^{31}P CP/MAS spectrum of polycrystalline **6b**, rotated at 11 kHz. Interestingly, ^{195}Pt satellites are visible close to the isotropic line, and the $^{1}J_{PPt}$ value (2685 Hz) is in good agreement with the solution data.

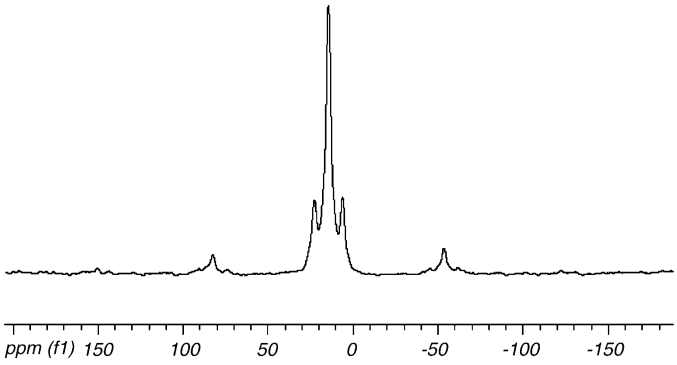

Fig. 5. ^{31}P CP/MAS spectrum of **6b** (161.9 MHz) at a rotational frequency of 11 kHz. The two peaks close to the isotropic line are ^{195}Pt satellites, the outer lines are rotational sidebands.

Two ^{13}C CP/MAS spectra of polycrystalline **6b** are illustrated in Fig. 6. The signals of the aliphatic carbons overlap (26 ppm), but they have rather small CSA values, such that even at the low spinning speed of 4 kHz there are no rotational sidebands. This indicates that the aliphatic chain is rather flexible and mobile even in the solid state. The ^{13}C signals of the phenyl carbon atoms at about 132 ppm (*ortho*, *meta*, and *para*) and 146 ppm (*ipso*) show however characteristically large CSA values with multiple sets of rotational sidebands.

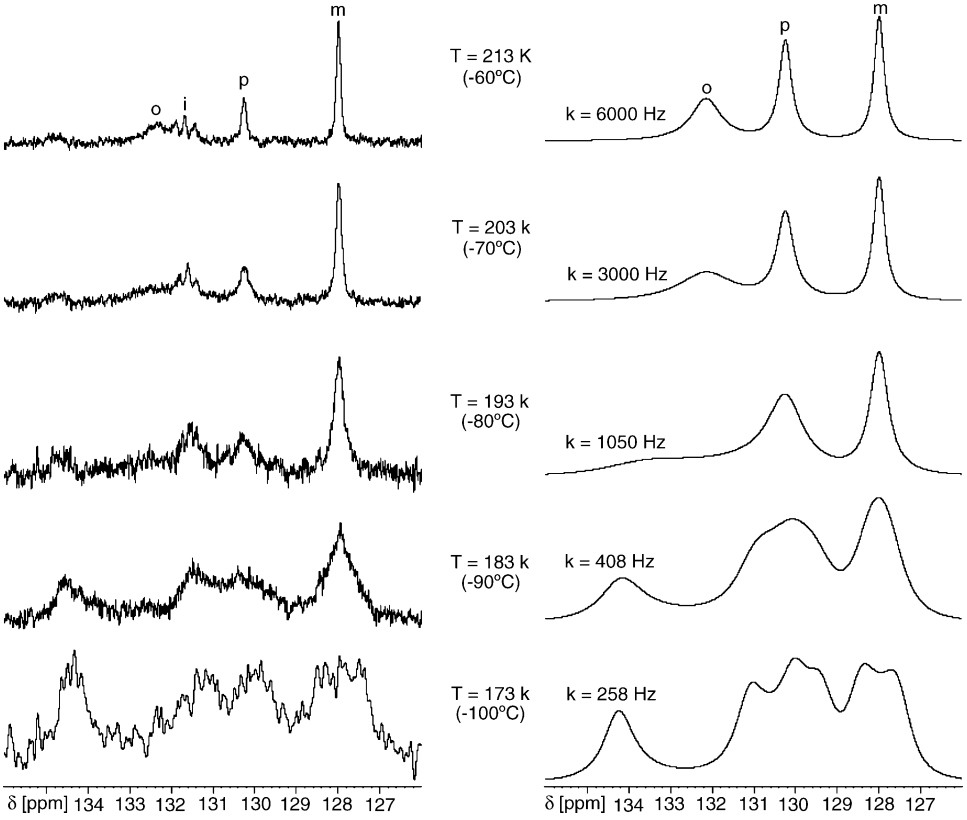

Fig. 4. ^{13}C NMR spectra of **6b** in $CDFCl_2$ (100.6 MHz, aromatic region only) at various temperatures. Left, experimental data; right, corresponding simulations.

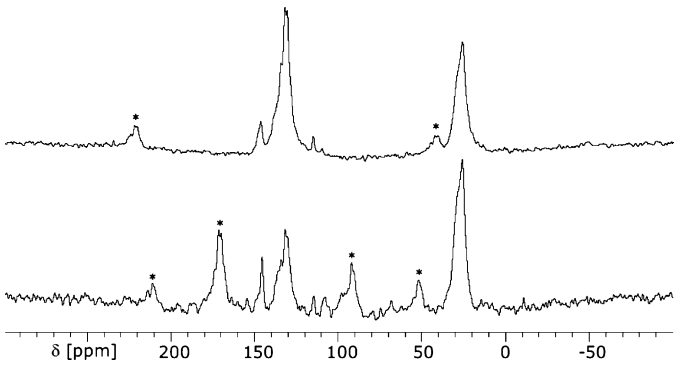

Fig. 6. ^{13}C CP/MAS spectra of polycrystalline **6b** (100.6 MHz) at rotational frequencies of 9 kHz (top trace) and 4 kHz (bottom trace). The asterisks denote rotational sidebands.

When **6b** was brought as a monolayer on a silica surface, the CSA values in the ^{31}P and ^{13}C CP/MAS spectra were not reduced, and identical signal patterns resulted. This is a clear indication that no adsorption on (or reaction with) the silica surface occurs, important information for the later use of such compounds as immobilized catalysts [15].

The ^{2}H CP/MAS spectrum of polycrystalline **6b**-d_2 is depicted in Fig. 7, together with a simulated lineshape [16]. In contrast to spectra of crystalline compounds with non-mobile ^{2}H nuclei, no "classical" Pake pattern is observed. The quadrupolar coupling constant can only be roughly estimated as between 6 and 15 kHz. Nonetheless, this indicates that the methylene chain in **6b**-d_2 is conformationally mobile, although the compound is crystalline with a high melting point near 200 °C. In view of the large size of the pentafluorophenyl ligand in Fig. 2, it is clear that the methylene chain cannot completely rotate about the metal center. Otherwise, the phenyl carbon signals (Fig. 7) would have displayed reduced CSA values. However, ca. 60° and 180° torsional motions about CH_2–CH_2–CH_2–CH_2 segments are feasible [17]. Comparing the lineshape in Fig. 7 with those obtained for hexane-d_{14} and decane-d_{22} [17], it can be concluded that the frequency of such conformational changes involving the CHD carbons of **6b**-d_2 is between 100 and 1000 kHz.

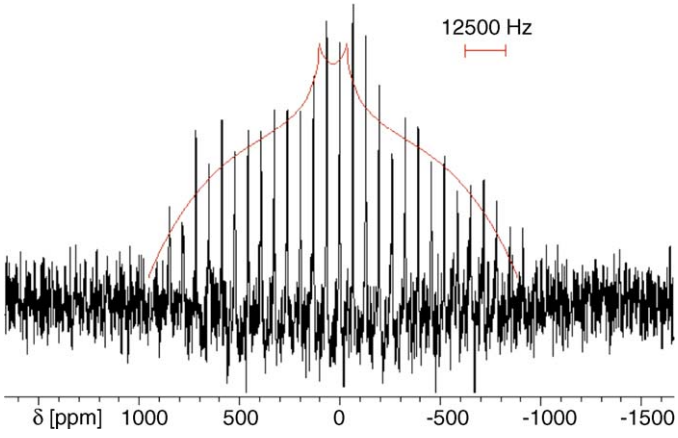

Fig. 7. ^{2}H CP/MAS spectrum of polycrystalline **6b**-d_2 (61.2 MHz) at a rotational frequency of 4 kHz. Smooth curve: simulated lineshape [16].

3. Discussion

The syntheses of the new complexes **4b**–**6b** in Scheme 4 proceed analogously to those of the lower and higher homologs described earlier (Scheme 2). However, several types of complementary data could be acquired. For example, the first crystal structure of a complex of the type **4** has been determined. As shown in Fig. 1, the substituents on the two phosphorus atoms in **4b** are eclipsed along the P–Pt–P axis (torsion angles ±3°). The two $(CH_2)_5CH{=}CH_2$ groups are *syn*, and extend on the same side of the platinum square plane. This conformation is ideal for ring-closing metathesis! Since we have been unable to provide rationales for the high yields obtained in these macrocyclizations, this prompts scrutiny for a previously unrecognized pre-organizational effect. However, we are presently unable to identify any molecule-based driving force for the observed conformation, and provisionally attribute it to a packing effect.

The first crystal structure of a complex of the type **5** has also been determined (Fig. 2). In the cases of 13-membered macrocycles such as (a) **5a** [3], (b) the analogous platinum complex with two $(CH_2)_4CH{=}CH(CH_2)_4$ bridges [4], and (c) the tris(alkene) precursor to the iron complex **2a** (Scheme 1) [5,18], alkene metathesis is highly selective for *E* C=C isomers. We suggest that $(CH_2)_4CH{=}CH(CH_2)_4$ bridges with *E* C=C linkages are better able to span *trans*-coordination sites. With longer and presumably less strained bridges, *E*/*Z* mixtures are obtained; there is often good evidence that *Z* isomers predominate [3]. In the case of **5b**, a 74:26 mixture of isomers is obtained. Although a definitive assignment is not possible from the NMR data, we suggest that the *Z* isomer dominates in accord with the crystal structure.

The conformation of the macrocycle in (*Z*)-**5b** shares certain features with those of **6a**,**c**,**e**–**f**. In all cases, the Pt–PPh_2–CH_2–CH_2 segments adopt gauche conformations, and the PPh_2–CH_2–CH_2–CH_2 segments *anti* conformations (as reflected by the torsion angles for (*Z*)-**5b** in Table 2). A rationale for the former, which is also believed to be favored in solution, has been proposed [3]. The PPh_2–*CH_2*–*CH_2*–*CH_2*–CH_2 segments in (*Z*)-**5b** exhibit gauche conformations, in contrast to those of **6c**–**e** and one of the two linkages in **6a**.

Attempts have been made to qualitatively correlate the crystal structures of **6a** and **c** to the rates of the exchange process in Scheme 3 [3]. The distances from the platinum atoms to the most remote macrocyclic carbon atoms are 5.62 and 7.83 Å, respectively. When the van der Waals radius of an sp^3 carbon atom is subtracted (1.70 Å), values that might be viewed as "bridge heights", 3.92 and 6.13 Å, are obtained. The platinum-chloride distances are ca. 2.36 Å, and when the van der Waals radius of the chlorine atom is added (1.78 Å), a "vehicle height" of 4.14 Å is obtained. With **6a**, the clearance is obviously not sufficient for the chloride ligand to pass under the macrocycle, whereas with **6c** it is ample.

Although a crystal structure of **6b** is not available, the distance from the platinum atom to the most remote macrocyclic carbon atom in (*Z*)-**5b** (6.21 Å) can be taken as an approximation. This translates to a "bridge height" of 4.51 Å for a "vehicle height"

of 4.14 Å. Empirically, the transit of the chlorine ligand through the macrocycle remains fast on the NMR time scale at room temperature. However, the clearance becomes low enough such that decoalescence can be observed at very low temperatures (Figs. 3 and 4) and activation parameters determined. Although this model is intuitive, it is vastly oversimplified, and it is important to emphasize that correlated conformational changes of the macrocycle are to be expected along the reaction coordinate.

In this regard, the solid-state NMR data verify the conformational mobility of the CH_2–CH_2–CH_2–CH_2 segments of the macrocycle. These facile solid-state torsional equilibria have major implications for the use of such complexes as molecular "compasses" [19] and related devices. Although the goal of this initial effort was to establish the feasibility of certain types of solid-state NMR measurements, it can be expected that the frequencies of torsional conformational changes will increase upon going from the smallest and presumably somewhat strained macrocycle **6a**–**6b** and then to **6c** and higher homologs. This will be tested with related complexes in future work.

In conclusion, this study has filled in important gaps regarding (1) syntheses of square-planar platinum complexes **6** with *trans*-spanning diphosphine ligands, (2) their dynamic properties, and (3) solid-state structures of cyclic and acyclic alkene-containing precursors to **6**. Future reports will describe new families of square-planar platinum and palladium complexes with *trans*-spanning ligands analogous to those in **2** [20].

4. Experimental

4.1. General data

All reactions were conducted in the absence of oxygen. Chemicals were treated as follows: THF, distilled from Na/benzophenone; CH_2Cl_2, distilled from CaH_2 (reactions) or simple distillation (chromatography); $ClCH_2CH_2Cl$ (99%, Fluka) and ethanol, used as received; $CDFCl_2$, prepared by a literature procedure [12]; $CDCl_3$, C_6D_6, THF-d_8 (3× Deutero GmbH or Eurisotop), $Br(CH_2)_5CH{=}CH_2$, $KPPh_2$ (2× Aldrich), Grubbs' catalyst, Wilkinson's catalyst (2× Strem), Pd/C (10%, Lancaster or Acros), and D_2 gas (Linde), used as received.

Solid-state NMR spectra were recorded on a digital Bruker Avance 400 NMR spectrometer equipped with a 4 mm MAS probehead. For the ^{31}P (^{13}C) CP/MAS measurements a contact time of 1 ms (5 ms), and a pulse delay of 10 s were applied. Polycrystalline $(NH_4)H_2PO_4$ (adamantane) was used as the Hartmann-Hahn and external chemical shift standard. The Hartmann-Hahn matching condition was established as previously described [21]. For ^2H CP/MAS spectra, a contact time of 5 ms with a 4 s pulse delay was applied. The 90° pulse length was 8.6 μs, as determined with perdeuterated poly(methylmethacrylate) (Deutero GmbH). The Hartmann-Hahn match was optimized using $P(p\text{-}C_6H_4D)_3$. Other spectra were recorded on standard modern instruments as described in previous papers [3,4]. Additional details are supplied elsewhere [11].

4.2. $PPh_2(CH_2)_5CH{=}CH_2$

A Schlenk flask was charged with $Br(CH_2)_5CH{=}CH_2$ (0.92 mL, 1.80 g, 10.2 mmol) and THF (14 mL), and cooled to −18 °C. Then $KPPh_2$ (0.5 M in THF, 20.3 mL, 10.2 mmol) was added dropwise with stirring. The mixture was stirred for 1 h, and then allowed to warm to room temperature. The solvent was removed by oil pump vacuum, and CH_2Cl_2 (3–6 mL) was added. The sample was chromatographed on silica gel (15 cm × 2.5 cm column; eluted with 1:2, v/v, CH_2Cl_2/hexanes). The solvent was removed from the product fraction by rotary evaporation and oil pump vacuum to give $PPh_2(CH_2)_5CH{=}CH_2$ as a clear oil (2.559 g, 9.06 mmol, 89%). Calc. for $C_{19}H_{23}P$:C, 80.82; H, 8.21. Found: C, 80.40; H, 8.35%.

NMR (δ, C_6D_6): ^1H (500.1 MHz) [22] 7.43 (t, $^3J_{HH}$ = 7 Hz, 4H of $2C_6H_5$), 7.08 (m, 6H of $2C_6H_5$), 5.70 (m, C*H*=CH_2), 4.96 (m, =CH_2), 1.93 (m, PCH_2), 1.88 (m, CH_2CH=), 1.41 (m, PCH_2CH_2), 1.28 (quintet, $^3J_{HH}$ = 8 Hz, $PCH_2CH_2CH_2$), 1.20 (quintet, $^3J_{HH}$ = 8 Hz, CH_2CH_2CH=); $^{13}C\{^1H\}$ (125.8 MHz) [22] 139.9 (d, $^1J_{CP}$ = 15.0 Hz, *i*-Ph), 139.0 (s, CH=), 133.1 (d, $^2J_{CP}$ = 18.8 Hz, *o*-Ph), 128.64 (d, $^3J_{CP}$ = 6.5 Hz, *m*-Ph), 128.59 (s, *p*-Ph), 114.6 (s, =CH_2), 34.0 (s, *C*H_2CH=), 31.0 (d, $^3J_{CP}$ = 12.5 Hz, $PCH_2CH_2CH_2$), 28.8 (s, *C*H_2CH_2C=), 28.5 (d, $^1J_{CP}$ = 12.8 Hz, PCH_2), 26.2 (d, $^2J_{CP}$ = 16.2 Hz, PCH_2CH_2); $^{31}P\{^1H\}$ (202.5 MHz) −16.8 (s).

IR (cm^{-1}, oil film) 3071 (m), 3054 (m), 2928 (s), 2854 (m), 2451 (w), 1884 (w), 1812 (w), 1640 (m), 1585 (w), 1481 (m), 1462 (w), 1431 (m), 1027 (m), 999 (m), 909 (s), 739 (s), 696 (s). MS[23] 283 (M^+ + H, 100%), 282 (M^+, 57%).

4.3. *trans*-$(Cl)(C_6F_5)Pt(PPh_2(CH_2)_5CH{=}CH_2)_2$ (**4b**)

A Schlenk flask was charged with $[Pt(\mu\text{-}Cl)(C_6F_5)(S(CH_2CH_2\text{–})_2)]_2$ (0.491 g, 0.505 mmol) [9], $PPh_2(CH_2)_5CH{=}CH_2$ (0.570 g, 2.02 mmol), and CH_2C1_2 (30 mL). The mixture was stirred (16 h) and the solvent was removed by oil pump vacuum. Then CH_2Cl_2 (1 mL) was added, followed by ethanol (6 mL). The sample was shaken, and a white solid precipitated. The sample was stored for several days at −30 °C. The supernatant was removed by pipette and the residue dried by oil pump vacuum to give **4b** as a white solid (0.780 g, 0.811 mmol, 80%), mp 110–116 °C.

NMR (δ, C_6D_6) [22]: ^1H (500.1 MHz) 7.55 (br s, 8H of $4C_6H_5$), 7.37–7.27 (br s, 12H of $4C_6H_5$), 5.73 (m, 2CH=), 5.01 (m, 2 =CH_2), 2.60 (m, 2PCH_2), 1.95 (m, $2PCH_2CH_2$ and $2CH_2$CH=), 1.25 (m, $2CH_2CH_2CH_2CH_2$CH=); $^{13}C\{^1H\}$ (125.8 MHz) [22,24,25] 138.9 (s, CH=), 133.5 (virtual t [10], $^2J_{CP}$ = 5.7 Hz, *o*-Ph), 131.5 (virtual t [10], $^1J_{CP}$ = 28.4 Hz, *i*-Ph), 130.4 (s, *p*-Ph), 128.4 (partially obscured by solvent signal, *m*-Ph), 114.7 (s, =CH_2), 33.9 (s, *C*H_2CH=), 31.0 (virtual t [10], $^3J_{CP}$ = 7.6 Hz, $PCH_2CH_2CH_2$), 28.7 (s, *C*H_2CH_2CH=), 26.4 (virtual t [10], $^1J_{CP}$ = 17.2 Hz, PCH_2), 25.7 (s, PCH_2CH_2); $^{31}P\{^1H\}$ (202.5 MHz) 16.1 (s, $^1J_{PPt}$ = 2656 Hz) [26]; ^{19}F (282.4 MHz) −118.8 (d, $^3J_{FF}$ = 23 Hz, $^3J_{FPt}$ = 402 Hz [26], *o*-C_6F_5), −165.5 (m, *m*- and *p*-C_6F_5).

IR (cm^{-1}, oil film) 3077 (m), 3050 (m), 2930 (s), 2855 (m), 1639 (m), 1501 (s), 1484 (m), 1463 (m), 1436 (s), 1103 (s), 1059

(s), 977 (m), 957 (s), 909 (m), 805 (s), 739 (s), 693 (s), 513 (s), 492 (s). MS [23] 961 (**4b**$^+$, 5%), 926 ([**4b**-Cl]$^+$, 100%), 759 ([**4b**-Cl-C_6F_5]$^+$, 18%), 477 ([**4b**-Cl-C_6F_5-Ph_2PR]$^+$, 37%), 282 (Ph_2PR^+, 67%).

4.4. *trans*-(Cl)(C_6F_5)Pt($PPh_2(CH_2)_5CH{=}CH(CH_2)_5PPh_2$) (*5b*)

A two-necked flask was charged with **4b** (0.165 g, 0.171 mmol), Grubbs' catalyst (0.004 g, 0.005 mmol), and CH_2Cl_2 (80 mL; the resulting solution is 0.0021 M in **4b**), and fitted with a condenser. The solution was refluxed. After 2 h, a second charge of Grubbs' catalyst was added (0.004 g, 0.005 mmol). After another 2 h, a third charge of Grubbs' catalyst was added (0.003 g, 0.004 mmol; 8 mol% total). After 1 h, the mixture was cooled to room temperature. The solvent was removed by rotary evaporation and oil pump vacuum. Then CH_2Cl_2 (1 mL) was added, followed by ethanol (4 mL). The mixture was swirled, and a white solid precipitated. The sample was concentrated to 2 mL and stored overnight at −30 °C. The supernatant was removed by pipette. The residue was washed with ethanol (4 mL) and dried by oil pump vacuum (1 day) to give **5b** as a white powder (0.135 g, 0.144 mmol, 84%) that was a 74:26 mixture of C=C isomers (tentatively assigned as *Z*/*E*; see text), mp 190–206 °C.

NMR (δ, C_6D_6): ^{1}H (500.1 MHz, major/minor) 7.46 (br d, $^3J_{HH}$ = 5.2 Hz, 8H of $4C_6H_5$), 7.31 (t, $^3J_{HH}$ = 7.3 Hz, 4H of $4C_6H_5$), 7.24 (t, $^3J_{HH}$ = 7.3 Hz, 8H of $4C_6H_5$), 5.45/5.62 (t, $^3J_{HH}$ = 4.9/3.8 Hz, CH=CH), 2.63 (br s, $2PCH_2$), 2.41 (br s, $2PCH_2CH_2$), 2.17/2.22 (m, $2CH_2CH$=), 1.60/1.60, 1.54/1.56 (2 m, $2CH_2CH_2CH_2CH$=); $^{13}C\{^1H\}$ (125.8 MHz, major isomer unless noted) [24,25] 132.6 (virtual t [10], $^2J_{CP}$ = 5.6 Hz, *o*-Ph), 132.2 (virtual t [10], $^1J_{CP}$ = 27.3 Hz, *i*-Ph), 130.4 (s, *p*-Ph), 130.18/130.14 (2 s, minor/major CH=CH), 128.0 (virtual t [10], $^3J_{CP}$ = 5.2 Hz, *m*-Ph), 30.9 (s, CH_2CH=), 29.5 (virtual t [10], $^3J_{CP}$ = 8.3 Hz, $PCH_2CH_2CH_2$), 28.3 (s, CH_2CH_2CH=), 26.9 (virtual t [10], $^1J_{CP}$ = 19.1 Hz, PCH_2), 25.4 (s, PCH_2CH_2); $^{31}P\{^1H\}$ (202.5 MHz) 16.4 (s, 74%), 15.6 (s, 26%); ^{19}F (282.4 MHz) −119.3 (m, *o*-C_6F_5), −165.3 (m, *m*- and *p*-C_6F_5).

IR (cm^{-1}, oil film) 2928 (m), 2853 (w), 1634 (br), 1502 (s), 1461 (s), 1447 (m), 1104 (s), 1061 (s), 957 (s), 805 (m), 740 (m), 694 (m). MS [23] 933 (**5b**$^+$, 17%), 898 ([**5b**-Cl]$^+$, 100%), 731 ([**5b**-Cl-C_6F_5]$^+$, 70%).

4.5. *trans*-(Cl)(C_6F_5)Pt($PPh_2(CH_2)_{12}PPh_2$) (*6b*)

A Schlenk flask was charged with **5b** (0.080 g, 0.086 mmol), 10% Pd/C (0.0089 g, 0.0089 mmol Pd), $ClCH_2CH_2Cl$ (4.5 mL), and ethanol (4.5 mL), flushed with H_2, and fitted with a balloon of H_2. The mixture was stirred for 96 h, during which time the balloon was periodically recharged with H_2. The mixture was filtered through Celite, and the solvent was removed by oil pump vacuum. Then CH_2Cl_2 (0.5 mL) was added, followed by ethanol (3 mL). The mixture was concentrated under vacuum until a precipitate began to form. The sample was stored overnight at −30 °C. The supernatant was removed by pipette. The residue was washed with ethanol and dried by oil pump vacuum (1 day) to give **6b** as a white powder (0.079 g, 0.084 mmol, 99%), mp 195–202 °C.

NMR (δ, C_6D_6): ^{1}H (500.1 MHz) [27] 7.55 (m, 8H of $4C_6H_5$), 6.92 (m, 12H of $4C_6H_5$), 2.57 (m, $2PCH_2$) [28], 2.43 (m, $2PCH_2CH_2$) [28], 1.58 (m, $2PCH_2CH_2CH_2CH_2CH_2$), 1.52 (m, $2PCH_2CH_2CH_2CH_2CH_2CH_2$); $^{13}C\{^1H\}$ [24,25,27] (125.8 MHz) 133.2 (virtual t [10], $^2J_{CP}$ = 5.5 Hz, *o*-Ph), 132.5 (virtual t [10], $^1J_{CP}$ = 27.0 Hz, *i*-Ph), 130.3 (s, *p*-Ph), 127.9 (partially obscured by solvent signal, *m*-Ph), 30.2 (virtual t [10], $^3J_{CP}$ = 8.1 Hz, $PCH_2CH_2CH_2$), 27.7 (s, $PCH_2CH_2CH_2CH_2$), 27.5 (virtual t [10], $^1J_{CP}$ = 17.4 Hz, PCH_2), 27.2 (s, $PCH_2CH_2CH_2CH_2CH_2CH_2$), 26.7 (s, $PCH_2CH_2CH_2CH_2CH_2$), 25.9 (s, PCH_2CH_2); $^{31}P\{^1H\}$ (202.5 MHz) 16.1 (s, $^2J_{PPt}$ = 2683 Hz) [26]; ^{19}F (282.4 MHz) −118.9 (d, $^3J_{FF}$ = 23 Hz, $^3J_{FPt}$ = 410 Hz [10], *o*-C_6F_5), −165.7 (m, *m*- and *p*-C_6F_5).

^{1}H NMR (δ, THF-d_8, 500.1 MHz): at 25 °C, 7.53 (dd, J_{HH} = 5.5, 12.3 Hz, 8H of $4C_6H_5$), 7.31 (t, $^3J_{HH}$ = 7.3 Hz, 4H of $4C_6H_5$), 7.24 (t, $^3J_{HH}$ = 7.4 Hz, 8H of $4C_6H_5$), 2.69 (m, $w_{1/2}$ = 23.1 Hz, $2PCH_2$), 2.33 (m, $w_{1/2}$ = 23.3 Hz, $2PCH_2CH_2$), 1.61 (br s, $w_{1/2}$ = 19.1 Hz, $2PCH_2CH_2CH_2CH_2CH_2$), 1.50 and 1.43 (2 s (2:1), $w_{1/2}$ = 10.5 and 10.5 Hz, $2PCH_2CH_2CH_2CH_2CH_2CH_2$); at −95 °C, 7.55 (br m, $w_{1/2}$ = 91.0 Hz, 8H of $4C_6H_5$), 7.37 (br m, $w_{1/2}$ = 24.7 Hz, 4H of $4C_6H_5$), 7.31 (br m, $w_{1/2}$ = 27.1 Hz, 8H of $4C_6H_5$), 2.70 (m, $w_{1/2}$ = 26.0 Hz, $2PCH_2$), 2.32 (m, $w_{1/2}$ = 39.5 Hz, $2PCH_2CH_2$), 1.61 (m, $w_{1/2}$ = 25.9 Hz, $2PCH_2CH_2CH_2CH_2CH_2$), 1.46 and 1.40 (2 s (2:1), $w_{1/2}$ = 18.5 and 18.5 Hz, $2PCH_2CH_2CH_2CH_2CH_2CH_2$).

IR (cm^{-1}, KBr pellet) 2929 (m), 2856 (w), 1630 (br), 1502 (s), 1461 (s), 1436 (m), 1261 (m), 1246 (m), 1103 (m), 1060 (m), 1000 (w), 957 (s), 805 (m), 740 (m), 693 (m), 512 (m). MS [23] 935 (**6b**$^+$, 23%), 900 ([**6b**-Cl]$^+$, 100%), 733 ([**6b**-Cl-C_6F_5]$^+$, 85%).

4.6. *trans*-(Cl)(C_6F_5)Pt($PPh_2(CH_2)_5CHDCHD(CH_2)_5PPh_2$) (*6b-d$_2$*)

This complex was prepared analogously to **6b** using either 10% Pd/C (some label scrambling, see text) or Wilkinson's catalyst.

^{2}H NMR (δ, C_6D_6, 61.4 MHz) 1.39 (m). MS [23] 938 (**6b**-d_2^+, 14%), 902 ([**6b**-d_2-Cl]$^+$, 91%), 735 ([**6b**-d_2-Cl-C_6F_5]$^+$, 40%).

4.7. Crystallography

Colorless irregular crystals of **4b** and (*Z*)-**5b** were obtained from ethanol/CH_2Cl_2. Data were collected as outlined in Table 1. Lorentz, polarization, and absorption (empirical, using SABABS (2.03) [29] and based upon the Laue symmetry of reciprocal space) corrections were applied. The structures were solved by direct methods (**4b**, Sir-97 [30]; (*Z*)-**5b**, XS [29]). The parameters were refined with all data by full-matrix-least-squares on F^2 using XL of the SHELXL (6.12) software package [29]. Non-hydrogen atoms were refined with anisotropic thermal parameters unless disordered. The

hydrogen atoms were fixed in idealized positions using a riding model. In **4b**, one set of PPh_2 rings and the *meta* and *para* C_6F_5 fluorine atoms were disordered between two sites that refined to 50:50 occupancy. The five terminal carbon atoms of the $(CH_2)_5CH{=}CH_2$ segments were disordered between two or more sites, the occupancies of which could not be refined.

CCDC-283900 (**4b**) and CCDC-283901 ((*Z*)-**5b**) contain the supplementary crystallographic data for this paper. These data can be obtained free of charge via http://www.ccdc.cam.ac.uk/conts/retrieving/html (or from the Cambridge Crystallographic Data Centre, 12 Union Road, Cambridge CB2 1EZ, UK; fax: (+44) 1223-336-033; or e mail: deposit@ccdc.cam.ac.uk).

Acknowledgments

We thank the Deutsche Forschungsgemeinschaft (DFG; SFB 623 (Heidelberg) and GL 300/1-3 (Erlangen) and Johnson Matthey PMC (platinum and ruthenium loans) for support, and Dr. Kai Hultzsch (Erlangen) for technical assistance.

References

[1] E.B. Bauer, J.A. Gladysz, in: R.H. Grubbs (Ed.), Handbook of Metathesis, vol. 2, Wiley–VCH, Weinheim, Germany, 2003, pp. 403–431.
[2] Lead references to contributions from other research groups:
(a) A.V. Chuchuryukin, H.P. Dijkstra, B.M.J.M. Suijkerbuijk, R.J.M. Klein Gebbink, G.P.M. van Klink, A.M. Mills, A.L. Spek, G. van Koten, Angew. Chem., Int. Ed. 42 (2003) 228;
A.V. Chuchuryukin, H.P. Dijkstra, B.M.J.M. Suijkerbuijk, R.J.M. Klein Gebbink, G.P.M. van Klink, A.M. Mills, A.L. Spek, G. van Koten, Angew. Chem. 115 (2003) 238;
(b) V. Martinez, J.-C. Blais, D. Astruc, Angew. Chem., Int. Ed. 42 (2003) 4366;
V. Martinez, J.-C. Blais, D. Astruc, Angew. Chem. 115 (2003) 4502;
(c) L.-E. Perret-Aebi, A. von Zelewski, C. Dietrich-Buchecker, J.-P. Sauvage, Angew. Chem., Int. Ed. 43 (2004) 4482;
L.-E. Perret-Aebi, A. von Zelewski, C. Dietrich-Buchecker, J.-P. Sauvage, Angew. Chem. 116 (2004) 4582.
[3] E.B. Bauer, F. Hampel, J.A. Gladysz, Organometallics 22 (2003) 5567.
[4] T. Shima, E.B. Bauer, F. Hampel, J.A. Gladysz, Dalton Trans. (2004) 1012.
[5] T. Shima, F. Hampel, J.A. Gladysz, Angew. Chem., Int. Ed. 43 (2004) 5537;
T. Shima, F. Hampel, J.A. Gladysz, Angew. Chem. 116 (2004) 5653.
[6] C.A. Bessel, P. Aggarwal, A.C. Marschilok, K.J. Takeuchi, Chem. Rev. 101 (2001) 1031.
[7] G.S. Kottas, L.I. Clarke, D. Horinek, J. Michl, Chem. Rev. 105 (2005) 1281.
[8] The exchange of H_a and H_b in Scheme 3 can be analyzed as follows. In both **I** and **II**, H_a and H_d are enantiotopic, as are H_b and H_c. H_a is diastereotopic with H_b and H_c. H_a in **I** exchanges with H_c in **II**, which is in turn chemical shift equivalent with enantiotopic H_b. Similarly, H_b in **I** exchanges with H_d in **II**, which is in turn chemical shift equivalent with enantiotopic H_a. The diastereotopic P*Ph*$_2$ groups (Ph_a, Ph_b) exchange analogously.
[9] R. Usón, J. Forniés, P. Espinet, G. Alfranca, Synth. React. Inorg. Met.-Org. Chem. 10 (1980) 579.
[10] W.H. Hersh, J. Chem. Educ. 74 (1997) 1485 (in the experimental section, the *apparent* couplings between adjacent peaks of the triplets are given).
[11] N. Lewanzik, Diplom Thesis, Ruprecht-Karls-Universität Heidelberg, 2004.
[12] J.S. Siegel, F.A.L. Anet, J. Org. Chem. 53 (1988) 2629.
[13] Available from Cherwell Scientific (http://www.cherwell.com) and other suppliers.
[14] T.M. Duncan, A Compilation of Chemical Shift Anisotropies, Farragut Press, Chicago, 1990.
[15] (a) C. Merckle, J. Blümel, Adv. Synth. Catal. 345 (2003) 584;
(b) C. Merckle, J. Blümel, Topics Catal. 34 (2005) 5;
(c) S. Reinhard, P. Šoba, F. Rominger, J. Blümel, Adv. Synth. Catal. 345 (2003) 589;
(d) S. Reinhard, K.D. Behringer, J. Blümel, New J. Chem. 27 (2003) 776;
(e) T. Posset, F. Rominger, J. Blümel, Chem. Mater. 17 (2005) 586;
(f) Y. Yang, J. Blümel, in preparation;
(g) A. Seifert, R. Fetouaki, J. Blümel, in preparation.
[16] D.J. McAdoo, C.E. Hudson, J. Am. Chem. Soc. 103 (1981) 7710.
[17] N. Nakaoka, T. Ueda, N. Nakamura, Z. Naturforsch. A 57 (2002) 435.
[18] The formation of the *E*,*E*,*E* Isomer has been confirmed crystallographically: L. Wang, F. Hampel, unpublished results, Universität Erlangen-Nürnberg, 2005.
[19] M.A. Garcia-Garibay, Proc. Natl. Acad. Sci. 102 (2005) 10771.
[20] A. Nawara, T. Shima, F. Hampel, J.A. Gladysz, J. Am. Chem. Soc. 128 (2006) 4962.
[21] S. Reinhard, J. Blümel, Magn. Reson. Chem. 41 (2003) 406.
[22] Definitive ^1H and ^{13}C NMR assignments for this compound were made using ^1H,^1H-COSY and ^1H,^{13}C-COSY spectra, as detailed elsewhere [11].
[23] *m/z* (FAB) for most intense peak of isotope envelope (relative intensity, %).
[24] The C_6F_5 carbon resonances were not observed. These require larger numbers of transients due to the fluorine and platinum couplings.
[25] The $PtPC_6H_5$ ^{13}C NMR assignments have abundant precedent. See for example:
P.W. Jolly, R. Mynott, Adv. Organomet. Chem. 19 (1981) 2571.
[26] This coupling represents a satellite (d; $^{195}Pt = 33.8\%$), and is not reflected in the peak multiplicity given.
[27] Definitive ^1H and ^{13}C NMR assignments for this compound were made using ^1H,^1H-COSY, ^1H,^{13}C-COSY, and HMBC spectra, as detailed elsewhere [11].
[28] The aliphatic ^1H NMR and ^{13}C NMR signals were assigned from a ^1H, ^{13}C COSY spectrum.
[29] G.M. Sheldrick, Bruker Analytical X-ray-Division, Madison, Wisconsin, 2001.
[30] A. Altomare, M.C. Burla, M. Camalli, G.L. Cascarano, C. Giacovazzo, A. Guagliardi, A.G.G. Moliterni, G. Polidori, R. Spagna, J. Appl. Cryst. 32 (1999) 115.